A REVIEW OF GROUNDWATER CONTAMINANT TRANSPORT MODELING TECHNIQUES

A REVIEW OF GROUNDWATER CONTAMINANT TRANSPORT MODELING TECHNIQUES

T.V. Hromadka II
Director of Water Resources Engineering, Williamson and Schmid, Irvine, CA 92714 and Professor, Department of Mathematics, University of California, Fullerton, CA 92634

ABSTRACT

The current technology of computer modeling groundwater contaminant transport involves widespread use of domain-discretized methods such as finite element and finite differences. Nodal Domain Integration or Control Volume methods are also used frequently due to the continuity of mass transport relationships. In this paper, some of the dominant underpinnings of these domain-discretized techniques are reviewed, and a uniformity between modeling techniques is presented. Because a principal variation between the numerical techniques is the capacitance matrix, the focal point in the comparison will address this term in the numerical analog.

INTRODUCTION

This paper introduces the reader to numerical modeling techniques that can be applied to the hydraulic analysis of groundwater flow and, by extension, groundwater contaminant transport. Numerical modeling techniques applied to mathematical models of groundwater flow imply the use of modern digital computers, which are now widely used for many engineering and scientific applications. Improvement in numerical techniques and computers now make it possible to solve rather complicated porous media flow problems on miniclass or even microclass computers.

Numerical models of regional groundwater flow have been widely used for a number of years to aid in aquifer management. Reviews of the basis and the use of such models can be found in Freeze and Cherry[4], Remson et al.[12], Pinder and Gray[11], and Bear[1]. Usually these models are two-dimensional models of the zone of saturation where the coordinates are oriented in the horizontal plane. The vertical direction is regarded as an integrated average where vertical velocity components are assumed to zero. Both the finite-element and finite-difference approaches are used as numerical analogs of the governing two-dimensional, dynamic equation of state. In several special cases, three-dimensional models have been advanced, and models that include the unsaturated zone have been developed. Contaminant transport submodels are overlayed upon the groundwater flow modeling results, using flow velocity estimates and estimate of soil water saturation.

Obtaining and applying a model that is already developed is sometimes difficult for several reasons. The most often encountered difficulty is that after a model is developed, verified, and applied there are inadequate resources for maintaining the model and servicing it. All modern software that is widely used requires a central enterprise for maintaining the software, usually the vendor. Second, numerical groundwater models, although elegantly constructed to solve the problem they are designed for, are oftentimes not truly user-oriented. Finally, another troublesome problem that may arise in adapting a model to a new environment is that sometimes models may be machine dependent. It is sometimes an unsurmountable task to adapt a model to a different computer from the one it was developed on. As a consequence, it may be more practical in some cases to start from scratch and build a new numerical model.

Notwithstanding these problems, numerical modeling, when combined with appropriate geotechnical exploration and hydrologic analyses, is a powerful tool. The use of existing numerical models or the development of a new model require some understanding of not only the physical and chemical processes involved in contaminant transport and groundwater movement but also of the basic mathematical principles needed to develop a numerical analog. This paper is designed to, in part, meet this need. Only a very limited treatment of numerical techniques is given here; the reader should consult the several referenced texts for additional information[1,4,11,12].

THE MATHEMATICAL PROBLEM

Both saturated and unsaturated flow processes must be evaluated to realistically model the hydraulic behavior of groundwater flow and contaminant transport. Similarly, introduction of contaminants into unconfined aquifers should include an analysis of unsaturated flow phenomena. Because this paper focuses upon the numerical modeling aspects, the groundwater flow component is examined for simplicity.

Consider the most complicated case first. To make the mathematical statement as simply as possible, we will assume a homogeneous nondeformable porous medium but will allow hydraulic conductivity to vary directionally (i.e., an anisotropic medium). We will not include a consideration of air flow; we will deal only with water flow. Continuity for a differential control volume may be expressed in Cartesian coordinates as

$$\frac{\partial v_x}{\partial x} + \frac{\partial v_y}{\partial y} + \frac{\partial v_z}{\partial z} = -\frac{\partial \theta}{\partial t} \tag{1}$$

where x, y, and z are Cartesian coordinates; t is time; v_x, v_y, and v_z are velocity fluxes in their respective directions; and θ is the volumetric moisture content. For simplicity, fluid sources and sinks are not included. Darcy's law is

$$v_x = -K_x \frac{\partial \phi}{\partial x}$$

$$v_y = -K_y \frac{\partial \phi}{\partial y} \tag{2}$$

$$v_z = -K_z \frac{\partial \phi}{\partial z}$$

where K_x, K_y, and K_z are the principal direction hydraulic conductivity coefficients and ϕ is the total hydraulic head where

$$\phi = \psi + h \tag{3}$$

where ψ is the pore water pressure head and h is the elevation head. If z is oriented vertically upward, $(h \equiv z)$. Equations (2) and (3) only apply to porous media flow where inertial forces are negligible (i.e., a Reynolds' number less than 3). Substituting, Equation (2) into Equation (1) yields

$$\frac{\partial \left[K_x \frac{\partial \phi}{\partial x} \right]}{\partial x} + \frac{\partial \left[K_y \frac{\partial \phi}{\partial y} \right]}{\partial y} + \frac{\partial \left[K_z \frac{\partial \phi}{\partial z} \right]}{\partial z} = \frac{\partial \phi}{\partial t} \tag{4}$$

To solve Equation (4), there must be a known relationship between θ and ψ. We have two options: we can replace $\frac{\partial \theta}{\partial t}$ with

$$\frac{\partial \theta}{\partial t} = \theta^* \frac{\partial \phi}{\partial t} \tag{5}$$

or replace ϕ on the left side with a function of θ, yielding the diffusion form of the equation. From a numerical standpoint it is usually better to modify the right-hand side of Equation (4), and leave Equation (4) with total head as the state variable. Equation (5) may exist, provided there is unique single-valued function θ^*, which is given by

$$\theta^* = \begin{cases} \dfrac{\partial \theta}{\partial \psi} & , \quad \psi < 0 \\ \\ 0 & , \quad \psi \geq 0 \end{cases} \tag{6}$$

The condition $(\psi < 0)$ represents unsaturated flow, and the condition $(\psi \geq 0)$ represents saturated flow. For unsaturated flow, we must know the functional form $(\theta = \theta(\psi))$, the so-called soil moisture characteristics that must be determined in the laboratory using soil samples or must be inferred from data, such as that published by Guymon et al.[6].

Furthermore, when $(\psi < 0)$, the hydraulic conductivity is a function of water content or pore water pressure; i.e., $(K = K(\psi))$ and this function must be determined by laboratory analysis of soil samples or inferred[5]. For unsaturated flow, Equation (4) is nonlinear since the hydraulic conductivity coefficients are functions of pore pressure head. As long as the temporal term exists, Equation (4) is a parabolic equation.

To solve Equation (4), we must have boundary and initial conditions. Generally, these are of the form

Boundary Conditions
$$\phi = \phi(s) \qquad , t > 0$$
$$\frac{\partial \phi}{\partial n} = q_n(s)/K_n \quad , t > 0 \tag{7}$$

Initial Condition
$$\phi = \phi_0(x,y) \qquad , t > 0$$

where s is a coordinate tangential to the solution domain surface, n is a normal coordinate to this surface, and $q_n(s)$ is a flux condition that may be negative, zero, or positive. The first boundary condition represents a specified hydraulic head along the boundary. Since it is permissible for this boundary condition to vary with distance along the boundary, it may be a function of distance, s. Also, the boundary condition may vary in time in a step function manner. The second boundary condition deals with a flux condition normal to the boundary surface. Oftentimes the hydrologist tries to locate a boundary so that the flux is zero. If, unfortunately, a flux condition does exist, estimates of flux normal to the boundary must be made by employing Darcy's law. This condition may vary as a function of distance along the boundary and may vary in time in some prescribed manner. Finally, it is usually the case that we have mixed boundary condition problems. A portion of a boundary may have a prescribed head while other portions may have a prescribed flux condition.

Most applications to groundwater flow and contaminant transport problems involve two-dimensional solutions. If we assume flow in the z direction is zero, y is vertically up and x is tangential to the earth's surface (horizontal), Equation (4) becomes

$$\frac{\partial(K_x \partial\phi/\partial x)}{\partial x} + \frac{\partial(K_y \partial\phi/\partial y)}{\partial y} = \theta^* \frac{\partial\phi}{\partial t} \tag{8}$$

which for unsaturated flow is a nonlinear parabolic partial differential equation. The total hydraulic head is now ($\phi \approx \psi + y$). Equations (5), (6), and (7) are required to solve Equation (8). For saturated flow, i.e., *the entire solution domain is saturated, Equation (8) becomes elliptic.* The right side of Equation (8) is identically zero. When the aquifer is homogeneous and isotropic, [$K_x = K_y$ and $K \neq f(x,y)$], it yields the well-known Laplace equation, which is independent of aquifer parameters; i.e.,

$$\nabla^2\phi = 0 \tag{9}$$

Only boundary conditions determine the solution of Equation (9).

If we again assume flow in the z direction is zero, but orient both the x and y coordinates in a plane tangential to the earth's surface, Equation (8) is correct for purely unsaturated flow; however, representing temporal variations for fully saturated flow, the right side *is not zero but becomes a function of total hydraulic head and storage* properties of the porous media:

$$\frac{\partial(T_x \partial\phi/\partial x)}{\partial x} + \frac{\partial(T_y \partial\phi/\partial y)}{\partial y} = S \frac{\partial H}{\partial t} \tag{10}$$

where H is the total saturated thickness (unconfined aquifer) or is equal to ϕ (confined aquifer), S is a storage coefficient, and T_x and T_y are the transmissibility coefficients that depend on H in the unconfined case. The storage coefficient is substantially different in the physical process it represents and in magnitude, depending on whether a confined aquifer or free water surface (unconfined) aquifer is being studied. We assume fluid velocity in the z direction is zero. This assumption (the Dupuit assumption) is reasonably true in fully confined aquifer problems and is only a rough approximation in unconfined aquifer problems. Again, Equation (10) is a nonlinear parabolic equation that requires boundary and initial conditions of the form of Equation (7) to solve for the state variable ϕ.

To this point, we have been using Cartesian coordinates to lay the framework for a mathematical model. Other forms of coordinates are useful also. For modeling direct introduction of contaminant, such as by injection, into a confined aquifer, cylindrical coordinates are the best to work with. If we assume ($K = K_x = K_y$), Equation (10) becomes *the linear one-dimensional equation (for the case of a homogeneous,* isotropic, confined aquifer):

$$\frac{\partial^2\phi}{\partial r^2} + \frac{1}{r}\frac{\partial\phi}{\partial r} = \frac{S}{K}\frac{\partial\phi}{\partial t} \tag{11}$$

where r is the radial coordinate from the well. We are assuming that velocities in their vertical direction are zero and that there is no movement of water in a circular direction around the well; i.e., water moves outward from the contaminant source along radial lines that look like the spokes of a wheel. To solve Equation (11), suitable boundary and initial conditions are required. One of the boundary conditions is at the well perimeter, where recharge rate or hydraulic head may be specified.

Now that we have developed several forms of equations describing porous media flow, we can conceptually consider the nature of the problem. Our approach has been to use physics-based laws or principles, and thus we have developed deterministic equations. That is, we have not considered probabilistic processes although by nature, porous media and soils are basically discrete. Freeze[5] has questioned our usual deterministic view of porous media flow. There is a wide statistical variation in the field parameters (e.g., hydraulic conductivity) that are included in our models. In spite of these uncertainties we will continue to take a deterministic view in this paper.

Although several special analytical solutions have been obtained for important groundwater flow problems, general solutions are usually required. This is particularly true for contaminant transport analysis. There are very few useful analytic solutions available for practical applications. As a consequence, the remainder of this section will present numerical analog techniques of which the most prominent are domain methods: finite differences or finite elements. Before discussing these, however, we will discuss some mathematical concepts that are useful to not only understanding numerical analogs but are essential to successfully applying these techniques.

The first concept is that of a solution domain. A solution domain for studying groundwater movement consists of a finite three-dimensional space of soil and water surrounded by a closed surface. The boundary of the solution domain is defined such that boundary conditions are known or can be reasonably inferred. For this reason, these types of problems are often referred to as boundary value problems, and the accurate specification of boundary conditions is an important part of the problem. Such a domain is shown in Figure 1. In this case, Equation (8) applies to the entire solution domain. An example of each type of boundary condition is shown; thus, for such a problem, the numerical analog must accommodate such conditions. Also shown is an internal interface condition requiring special numerical considerations since at this interface a parabolic equation (unsaturated zone) becomes an elliptic equation (saturated zone).

Upon defining a solution domain, initial conditions must be specified. Such conditions are usually specified at discrete points in the solution domain. These points are dictated by the discretization required in order to develop a general numerical solution, the second important concept. Figure 2 shows an example solution domain that has been discretized into subdomains. This example depicts a typical finite element solution. This example assumes that more accuracy is required where subdomains are small. Consequently, a particular numerical method may be required. Also notice that the solution boundary will involve some geometric approximation. In this case straight line segments approximate the solution boundary geometry. The discretization assumes lumped average parameters are available for each subdomain. This may not be the case, requiring calibration of the model before it can be applied to a case study. All models require some level of calibration if they are to yield useful results.

FINITE-DIFFERENCE METHOD

A finite-difference scheme can be constructed by discretization of the total solution domain and application of Darcy's law, Equation (2), and continuity. We will take this simple approach here, applying the method to a two-dimensional horizontal aquifer. By using finite-difference approximations for the flow equation, Equation (10), a numerical model can be developed that may include the effects of recharge or accretion. In the model, the soil matrix is assumed nondeformable and fluid compressibility effects are assumed negligible. The spatial variation of all parameters are assumed to be negligible in the vertical direction and linear in the horizontal (x,y) directions.

Since the soil-water is assumed incompressible, a volumetric control volume balance can be made, equating inflow of soil-water across a control volume boundary, Γ, to the rate of increase of soil-water content in the control volume, Ω. Figure 3 shows a typical control volume, Ω, with boundary ($\Gamma = \Gamma_1 + \Gamma_2 + \Gamma_3 + \Gamma_4$). In the finite-difference model, the groundwater basin is approximated by a mesh constructed of lines parallel to either the x or y axis.

At the center of each resulting control volume is a nodal point, $P_{i,j}$. From Figure 3, the control volume balance is given by

$$\Delta Y \left(-K_x h \frac{\partial \phi}{\partial x} \right)\Big|_{\Gamma_3} - \Delta Y \left(-K_x h \frac{\partial \phi}{\partial x} \right)\Big|_{\Gamma_1} + \Delta X \left(-K_y h \frac{\partial \phi}{\partial y} \right)\Big|_{\Gamma_4}$$

$$-\Delta X \left(-K_y h \frac{\partial \phi}{\partial y} \right)\Big|_{\Gamma_2} + (R\Delta X\Delta Y)\Big|_{\Omega} = \Delta X\Delta Y \left(S \frac{\partial \phi}{\partial t} \right)\Big|_{\Omega} \qquad (12)$$

where R is a soil-water volumetric source per unit ground surface area, assumed uniform on Ω; and S is the apparent specific yield that expresses the instantaneous volumetric soil-water removal (or addition) to the change in the volume of the aquifer below the water table.

In Equation (12), the soil water flow rate terms are defined on the boundaries of Ω, which are located midway between nodal points. Additionally, the volumetric rate of soil-water flow into Ω is determined by the Darcian flow rate multiplied by the cross-sectional area of flow, which depends on the width (Δx or Δy) and the height of the water table, h, above the impermeable underlying base.

A numerical solution can be determined by approximating the space derivatives at the midpoint and time derivatives for a small duration of time, recalculating transmissibility parameters based on the new estimates of the model variables, and then repeating the approximation procedure. The various rate and volumetric equations that are applicable to each control volume are simplified by assuming

$$\Delta Y \left(-K_x h \frac{\partial \phi}{\partial x} \right)\Big|_{\Gamma_3} = \Delta Y \left(-K_x h \frac{\partial \phi}{\partial x} \right)\Big|_{(x_0 - \frac{\Delta X}{2}, y_0)} \qquad (13a)$$

$$(R\Delta X\Delta Y)\Big|_{\Omega} = \Delta X\Delta Y R\Big|_{(x_0, y_0)} \qquad (13b)$$

$$\Delta X\Delta Y \left(S \frac{\partial \phi}{\partial t} \right)\Big|_{\Omega} = \Delta X\Delta Y \left(S \frac{\partial \phi}{\partial t} \right)\Big|_{(x_0, y_0)} \qquad (13c)$$

where (x_0, y_0) are the coordinates of nodal point, $P_{i,j}$ and all parameters are held constant for a specified period. The simplified equations are approximated by finite differences, as follows:

$$- \Delta Y \left[K_x h \frac{\partial \phi}{\partial x} \right]\Bigg|_{(x_0 - \frac{\Delta X}{2}, y_0)}$$

$$= - \frac{\Delta Y}{2} \left[(K_x h)\Big|_{P_{i-1,j}} + (K_x h)\Big|_{P_{i,j}} \right] \frac{(\phi_{i,j} - \phi_{i-1,j})}{\Delta X} \quad (14a)$$

$$\Delta X \Delta Y R \Bigg|_{(x_0, y_0)} = \Delta X \Delta Y R_{i,j} \quad (14b)$$

$$\Delta X \Delta Y \left[S \frac{\partial \phi}{\partial t} \right]\Bigg|_{(x_0, y_0)} = \Delta X \Delta Y S_{i,j} \frac{(\phi^{k+1} - \phi^k)}{\Delta t} \quad (14c)$$

In Equation (14), $R_{i,j}$ and $S_{i,j}$ are parameters evaluated at nodal point $P_{i,j}$. In (14c), the superscript k indicates values of the variable, ϕ, evaluated at time ($t = k\Delta t$), where Δt is some timestep size. It should be noted that the finite-difference approximations are based on the assumption that all parameters vary linearly *between nodal points*; consequently, other approximations can be developed assuming more complex variations of the model parameters.

The numerical algorithm is to first estimate all parameters based on *the known values of ϕ (and h) at some time level* ($t = k\Delta t$). If ($k = 0$), then the model time is zero and all values of ϕ are to be defined by the initial condition of the problem. The second step of the algorithm is to compute values of the variables ϕ^{k+1} from the several nodal equations developed by applying Equation (14) to each nodal point in the problem *domain*. The *third step* is to recompute the various parameters and the groundwater table depths, h, at each nodal point based on the new values of ϕ, and then proceed to steps one and two.

From Equation (14), a nodal equation can be written as

$$- C_1 \frac{(\phi_{i+1,j} - \phi_{i,j})}{\Delta X} \Delta Y + C_3 \frac{(\phi_{i,j} - \phi_{i-1,j})}{\Delta X} \Delta Y - C_2 \frac{(\phi_{i,j+1} - \phi_{i,j})}{\Delta Y} \Delta X$$

$$+ C_4 \frac{(\phi_{i,j} - \phi_{i,j-1})}{\Delta Y} \Delta X + R_{i,j} \Delta X \Delta Y = S_{i,j} \frac{(\phi_{i,j}^{k+1} - \phi_{i,j})}{\Delta t} \Delta X \Delta Y \quad (15)$$

where the coefficients (C_1, C_2, C_3, C_4) follow from Equation (14a). Rewriting Equation (15) with respect to nodal point values of ϕ gives

$$\phi_{i,j} \left[C_1 \frac{\Delta y}{\Delta x} + C_2 \frac{\Delta x}{\Delta y} + C_3 \frac{\Delta y}{\Delta x} + C_4 \frac{\Delta x}{\Delta y} \right] + \phi_{i-1,j} \left[- C_3 \frac{\Delta y}{\Delta x} \right]$$

$$+ \phi_{i+1,j} \left[- C_1 \frac{\Delta y}{\Delta x} \right] + \phi_{i,j-1} \left[- C_4 \frac{\Delta x}{\Delta y} \right] + \phi_{i,j+1} \left[- C_2 \frac{\Delta x}{\Delta y} \right]$$

$$+ R_{i,j} \Delta X \Delta Y = S_{i,j} \Delta X \Delta Y \frac{(\phi_{i,j}^{k+1} - \phi_{i,j}^k)}{\Delta t} \quad (16)$$

Applying Equation (16) to each nodal point in a n-nodal point mesh of the problem domain results in a system of n-linear equations that can be written in matrix form as

$$\underline{C} \, \underline{\phi} + \underline{R} = \underline{S} \, \underline{\dot{\phi}} \quad (17)$$

where $\underline{C}$ is the global matrix of coefficients from Equation (16); $\underline{R}$ and $\underline{S}$ are arrays using parameters describing a source flow rate and apparent specific yield at the nodal points; and $\underline{\phi}$ and $\underline{\dot{\phi}}$ are nodal point values, and the time derivative of nodal point values defined by

$$\underline{\dot{\phi}} = \frac{1}{\Delta t} (\underline{\phi}^{k+1} - \underline{\phi}^k) \quad (18)$$

For groundwater basin modeling problems where the water table varies slowly, the $\underline{C}$, $\underline{R}$, and $\underline{S}$ arrays are computed based on the values of ϕ at timestep k. *To better estimate the water table gradients*, however, the ϕ vector contribution may be computed as an implicit expression giving

$$\underline{C}[(1 - \epsilon) \, \underline{\phi}^k + \epsilon \, \underline{\phi}^{k+1}] + \underline{R} = \underline{S} \, (\underline{\phi}^{k+1} - \underline{\phi}^k)/\Delta t \quad (19)$$

where ($0 \leq \epsilon \leq 1$). For ($\epsilon = 0$), an explicit algorithm results. For ($\epsilon = 1$), a fully implicit algorithm results. For $\epsilon = 1/2$), the well-known Crank-

Nicolson algorithm results. Stability and convergence criteria for the various time-domain solution techniques are discussed in McWhorter and Sunada[9]. Equation (19) can be rewritten into the more convenient form

$$[\epsilon \underset{\sim}{C} - \underset{\sim}{S}/\Delta t]^k \phi^{k+1} = [(\epsilon - 1)\underset{\sim}{C} - \underset{\sim}{S}/\Delta t]^k \phi^k - \underset{\sim}{R}^k, 0 \le \epsilon \le 1 \quad (20)$$

The superscript notations on the parameter arrays indicate that values are calculated at timestep k. The matrix system of Equation (20) can be solved by iteration or the Gaussian elimination method to solve for ϕ^{k+1}. In Equation (20), the constant head boundary conditions are specified in setting

$$\phi_{i,j}^{k+1} = \phi_{i,j}^k = \phi_{i,j} \quad \text{(boundary condition)} \quad (21)$$

FINITE-ELEMENT METHOD

The finite-element method is now widely used to solve regional aquifer problems posed in a horizontal two-dimension scale as well as vertical slice two-dimensional scales. Bear[1] and Pinder and Gray[11] review some of these efforts. Some authors perceive several advantages to the use of finite-element methods over classical finite-difference methods. The most often cited are the following:

1. Ease of using a variable arbitrary discretization mesh
2. Ease of incorporating boundary conditions without special gradient approximations
3. Ease of dealing with heterogeneous-anisotropic domains

There are two basic ways of developing a finite-element numerical analog: the variational functional technique or the Galerkin technique. Both methods lead to identical results for the type of symmetric problems we are dealing with here. Because the Galerkin technique is somewhat more general and is widely cited by those applying finite element methods to porous media flow problems, we shall base our development on this method.

The Galerkin finite element technique is basically a rule for reducing the governing partial differential equations to a matrix statement involving a matrix of known elements and a matrix of unknown state variables. The Galerkin formulation solves the governing partial differential equation by setting the governing equation orthogonal to some error weighting function:

$$\int (B(\phi) - f)w = 0 \quad (22)$$

where B is a partial differential operator (operating on the variable ϕ). f is some function, and w is a weighting function. Since the horizontal two-dimensional problem was studied in the previous section, the vertical slice problem will be considered here. Using Equation (8) as the governing equation, Equation (22) becomes, on substituting Equations (8) and (5),

$$\int_{\Omega^e} \left[\partial \frac{(k_x \partial\phi/\partial x)}{\partial x} + \partial \frac{(k_y \partial\phi/\partial y)}{\partial y} - \theta^* \frac{\partial\phi}{\partial t} \right] N_j d\Omega = 0 \quad (23)$$

where e represents a particular finite element domain Ω^e and w equals N_j.

The next step is to define a finite element shape, which may range from triangles to quadrilateral shapes with special curved sides to geometrically simulate the boundary. In this derivation we will illustrate the finite-element method by using the commonly used triangle (shown in Figure 4). Finally, we make an assumption approximating the state variable within this domain and on its boundary; i.e., we specify a trial solution function such that

$$\hat{\phi} = \sum N_j \phi_j^e \quad (24)$$

where $\hat{\phi}$ approximates ϕ, ϕ_j^e are the nodal values, and N_j is a shape function. For simplicity we shall assume N_j is a linear polynomial function of space, requiring three vertex nodal points in triangular finite element Ω^e.

Equation (23) is integrated by parts, Equation (24) is substituted into the results, and the indicated differentiations and integrations are carried out over element Ω^e, yielding the element matrix equation

$$\underset{\sim}{S}^e \{\phi\}^e + \underset{\sim}{P}^e \{\dot{\phi}\}^e = 0 \quad (25)$$

where element matrices are given by

$$S^e = \frac{k_x^e}{4A^e} \begin{bmatrix} (y_{23}^2) & -(y_{13}y_{23}) & (y_{12}y_{23}) \\ & (y_{13}^2) & -(y_{12}y_{13}) \\ \text{symmetrical} & & (y_{12}^2) \end{bmatrix}$$

$$+ \frac{k_y^e}{4A^e} \begin{bmatrix} (x_{23}^2) & -(x_{13}x_{23}) & (x_{12}x_{23}) \\ & (x_{13}^2) & -(x_{12}x_{13}) \\ \text{symmetrical} & & (x_{12}^2) \end{bmatrix} \quad (26)$$

where $(y_{i,j} = y_j - y_i)$ and $(x_{i,j} = x_j - x_i)$ and

$$P^e = \frac{(\theta^*)^e A^e}{12} \begin{bmatrix} 2 & 1 & 1 \\ 1 & 2 & 1 \\ 1 & 1 & 2 \end{bmatrix} \qquad (27)$$

and $\{\phi\}^e$ is a vector of nodal state variables, $\{\dot{\phi}\}^e$ is a vector of nodal state variable derivatives with respect to time, and A^e is the element area. Zienkiewicz[15] gives complete details on the derivation of element matrices and useful matrix formula. Each element matrix is a function of lumped element *parameters and the global coordinates of* its nodes. In order to carry out the required integrations, it is assumed that the parameters are constant in each element. Equation (25) is strictly applicable to interior elements or where there are no specified element boundary conditions.

The next step after deriving the completely general element *matrix equations is* to assemble each element matrix equation into the global system equation:

$$S\{\phi\} + P\{\dot{\phi}\} = \{F\} \qquad (28)$$

where S and P are square-banded system matrices that are functions of the element conduction and storativity parameters and spatial discretization, $\{\phi\}$ and $\{\dot{\phi}\}$ are vectors of the unknown state variable and its time derivative, respectively, and $\{F\}$ is a function of specified boundary conditions.

Algorithms for assembly of the system matrices, Equation (28), are given in several texts: Zienkiewicz[15], Myers[10], and Segerlind[13]. Generally, the approach in a computer program is to initialize the matrices to zero and then add in each element contribution in a way *such that each node equation will have all of the element contributions* accounted for. Specified boundary conditions are conveniently handled by entering the boundary condition in $\{F\}$ at the appropriate node number level, entering a 1 on the diagonal of S, and zeroing out all the other matrix elements contributing to that node equation. Natural boundary conditions, i.e., *zero flux conditions, are automatically* accommodated without any special provisions. Flux boundary conditions are entered into $\{F\}$ as described in Myers[10].

A general finite-difference formulation of the temporal term in Equation (28) is given by

$$\left[\frac{1}{\Delta t}P + \epsilon S\right]\phi^{t+\Delta t} = \left[\frac{1}{\Delta t}P - (1-\epsilon)S\right]\phi^t + \epsilon F^{t+\Delta t} + (1-\epsilon)F^t \qquad (29)$$

where Δt is a specified timestep. For $(\epsilon = 1/2)$, the *Crank-Nicolson* method results, for $(\epsilon = 1)$ a fully implicit method results, and for $(\epsilon = 0)$ a fully explicit method results. The horizontal two-dimensional problem model can be developed by following the previous derivation and using the appropriate governing flow equation.

Computer programs written for the finite element method are *commonly written in* FORTRAN language. Full advantage of the symmetrical, banded nature of the system matrices is taken to minimize computer memory requirements and to maximize the solution speed. Matrix solutions are generally by Gaussian elimination.

An excellent example of applying the finite element method of analysis is a study of water level and water quality effects of in the Coachella Valley, California[14]. This area is characterized by a large, unconfined groundwater basin in the desert region of southern California in the vicinity of Palm Springs. The approach taken was to use an *existing two-dimensional model and apply it to the horizontal* movement of water in the aquifer. Figure 5 shows the area modeled, which is surrounded by nonwater-bearing deposits. This particular model uses isoparametric quadrilateral elements, which are also shown in Figure 5. Isoparametric elements are simply a parametric algebraic formulation to transform *nonrectangular elements into rectangles for* purposes of the finite-element formulation.

Substantial efforts were required to identify boundary conditions and basin surface element inputs (e.g., artificial recharge) or outputs (e.g., pumpage). Calibration of the model was required *(always the case)* since imperfect knowledge of transmissive and storage *parameters was available.* This was done using historical data on inputs, outputs, boundary conditions, and measured water levels. Figure 6 shows a comparison of simulated and measured water levels at three points in the basin after calibration was completed.

UNIFIED DOMAIN METHODS

Hromadka and Guymon[7] and Hromadka et al.[8] have shown that an infinity of domain methods may be accommodated by a *single mass* lumping matrix system. This method, which is called Nodal Domain *Integration, stems from the same concept as the* Galerkin weighted residual method. A Galerkin finite-element formulation is obtained by defining an element shape and trial function and integrating over the finite element domain. Other mass lumping schemes can be devised by redefining the integration domain and the density of the state variable

approximation. For example, assuming a triangular element linear trial function and integrating over a subdomain, Ω_j, defined geometrically as one third of a finite-element area drawn to include one vertex as shown in Figure 7, an integrated finite-difference scheme is obtained. Depending on the domain of definition or the assumed trial function, an infinity of mass lumping numerical analogs may be obtained.

Similar to the finite element method, a general matrix equation may be defined

$$S^e\{\phi\}^e + P^e\{\dot{\phi}\}_e = \{F\} \tag{30}$$

where for a linear trial function, triangular finite element S is defined by Equation (26) and

$$P^e = \frac{(\theta^*)^e A^e}{3(\eta+2)} \begin{bmatrix} \eta & 1 & 1 \\ 1 & \eta & 1 \\ 1 & 1 & \eta \end{bmatrix} \tag{31}$$

where, as before, e represents a particular interior finite element, A^e is the element area, and $(\theta^*)^e$ is the element term defined by Equation (6). For ($\eta = 2$), the usual Galerkin finite-element formulation is obtained. For ($\eta = 22/7$) (approximately π), a subdomain integration formulation is obtained. For ($\eta \to \infty$), an integrated finite difference scheme results.

Thus a single computer code can be developed that encompasses all these domain numerical analogs. Through the specification of a single parameter, η, one can choose a numerical scheme that best fits the type of problem being considered. For instance, where the state variable, ϕ, may be changing slowly in space, specification of ($\eta = 2$) may be best. Where sharp wetting fronts occur in the solution domain, the specification of a large η (say 1,000) may be more appropriate. There is no reason why η may not be a function of space and time, permitting one the luxury of having the "best" numerical analog approximation in various subdomains of the solution region or where conditions may change with time. Time domain solutions are similar to those used in finite-element solutions (i.e., Equations (29)).

An example of the nodal domain integration method applied to an groundwater movement problem is presented in Figure 8. The solution domain consists of a two-dimensional vertical slice of soil containing several semi-pervious clay lenses. Figure 8 shows the solution domain divided into triangular elements (approximately 10 ft high by 30 ft wide). Ponded water in an flood control basin located near a landfill site tends to move horizontally in pervious layers rather than to percolate vertically to the underlying groundwater aquifer. Water is ponded to a 20-ft depth for 30 days. This example demonstrates the

need for good geotechnical data as well as a mathematical model simulation to verify the assumed hydraulic behavior of groundwater flow and contaminant flow. The model includes both saturated and unsaturated flow phenomena. The time domain solution is by the fully implicit technique to accommodate internal free water surface (phreatic) conditions. For this example η was set to 1,000.

REFERENCES

1. Bear, J., Hydraulics of Groundwater, McGraw-Hill International, Israel, 1979.

2. Freeze, R.A., 1971, Three-Dimensional, Transient, Saturated-Unsaturated Flow in a Groundwater Basin, Water Resources Research 7, pp. 347-366.

3. Freeze, R.A., 1975, A Stochastic Conceptual Analysis of One-Dimensional Groundwater Flow in Non-Uniform Homogeneous Media, Water Resources Research 11, pp.725-741.

4. Freeze, R.A., and Cherry, J.A., Groundwater, Prentice-Hall, Englewood Cliffs, N.J.: Prentice-Hall, 1979.

5. Guymon, G.L., Berg, R.L., Johnson, T.C., and Hromadka II, T.V., 1984, Mathematical Model of Frost Heave in Pavement," U.S. Army Cold Regions Research and Engineering Laboratory.

6. Guymon, G.L., Harr, M.E., Berg, R.L., and Hromadka II, T.V., 1981, A Probabilistic-Deterministic Analysis of One-Dimensional Ice Segregation in a Freezing Soil Column, Cold Regions Science and Technology 5, pp. 127-140.

7. Hromadka II, T.V., 1982, Nodal Domain Integration Model of One-Dimensional Advection-Diffusion, Advances in Water Resources 5, pp. 9-16.

8. Hromadka II, T.V., Guymon, G.L., and Pardoen, G.C., 1981, Nodal Domain Integration Model of Unsaturated Two-Dimensional Soil-Water Flow: Development, Water Resources Research 17, pp. 1425-1430.

9. McWhorter, D.B., and Sunada, D.K., Ground-Water Hydrology and Hydraulics, Water Resources Publications, Colorado, 1977.

10. Myers, G.E., Analytical Methods in Conduction Heat Transfer, McGraw-Hill, New York, 1971.

11. Pinder, G.F., and Gray, W.G., Finite Element Simulation in Surface and Subsurface Hydrology, Academic Press, New York, 1977.

12. Remson, I., Hronberger, G.M., and Molz, F.J., Numerical Methods in Subsurface Hydrology, Wiley-Interscience, New York, 1971.

13. Segerlind, L.J., Applied Finite Element Analysis, Wiley, New York, 1976.

14. Swain, L.A., 1977, Predicted Water-Level and Water-Quality Effects of Artificial Recharge in the Upper Coachella Valley, California, Using a Finite-Element Digital Model, U.S. Geological Survey, Water Resources Investigations No. 77-29, p. 54.

15. Zienkiewicz, O.C., The Finite Element Method, McGraw-Hill, London, 1977.
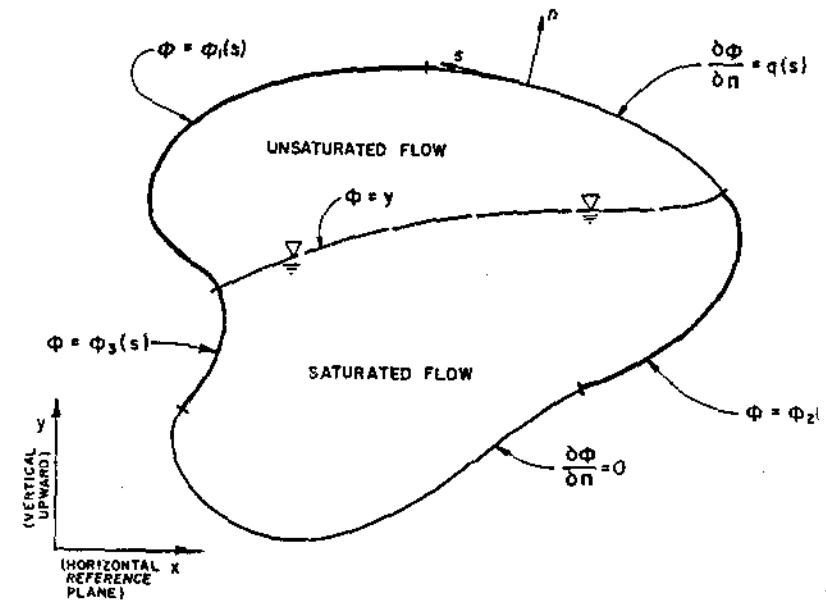
Figure 1. Example solution domain showing boundary condition forms and an internal interface condition.
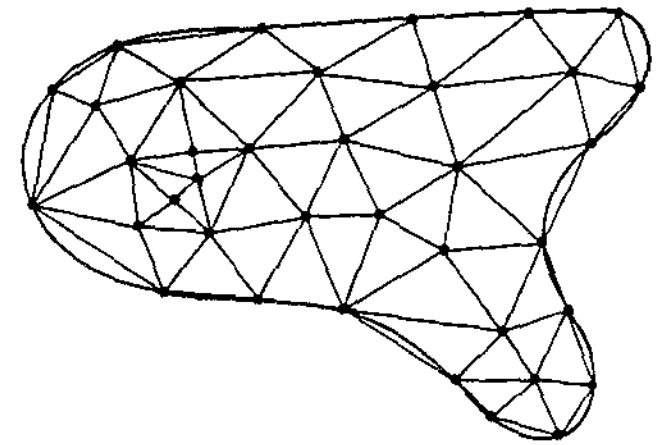
Figure 2. Discretization of solution domain.
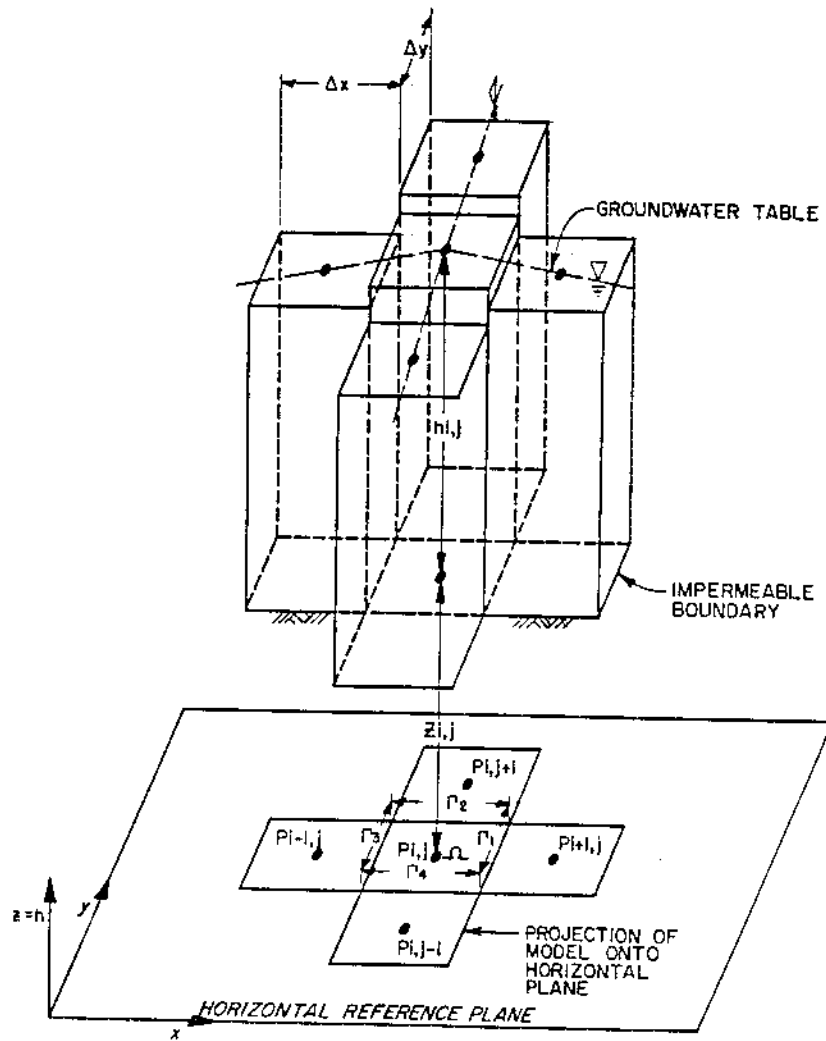
Figure 3. Finite-difference discretization scheme.
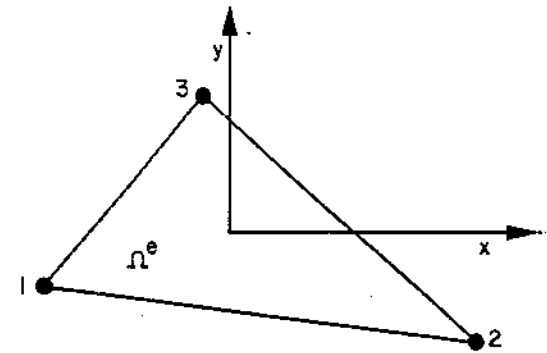
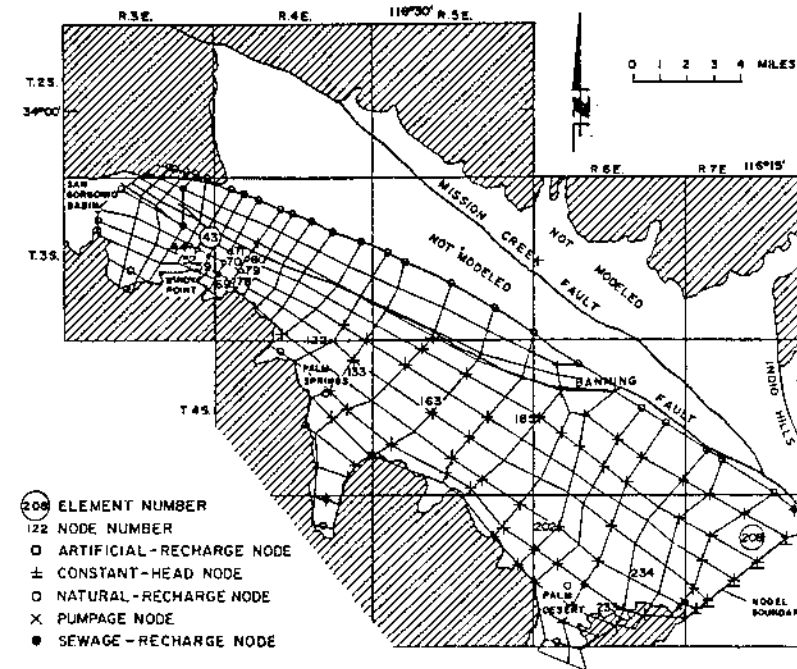
Figure 4. Finite-element triangle.

Figure 5. Finite-element layout for Upper Coachella Valley groundwater basin model[14].
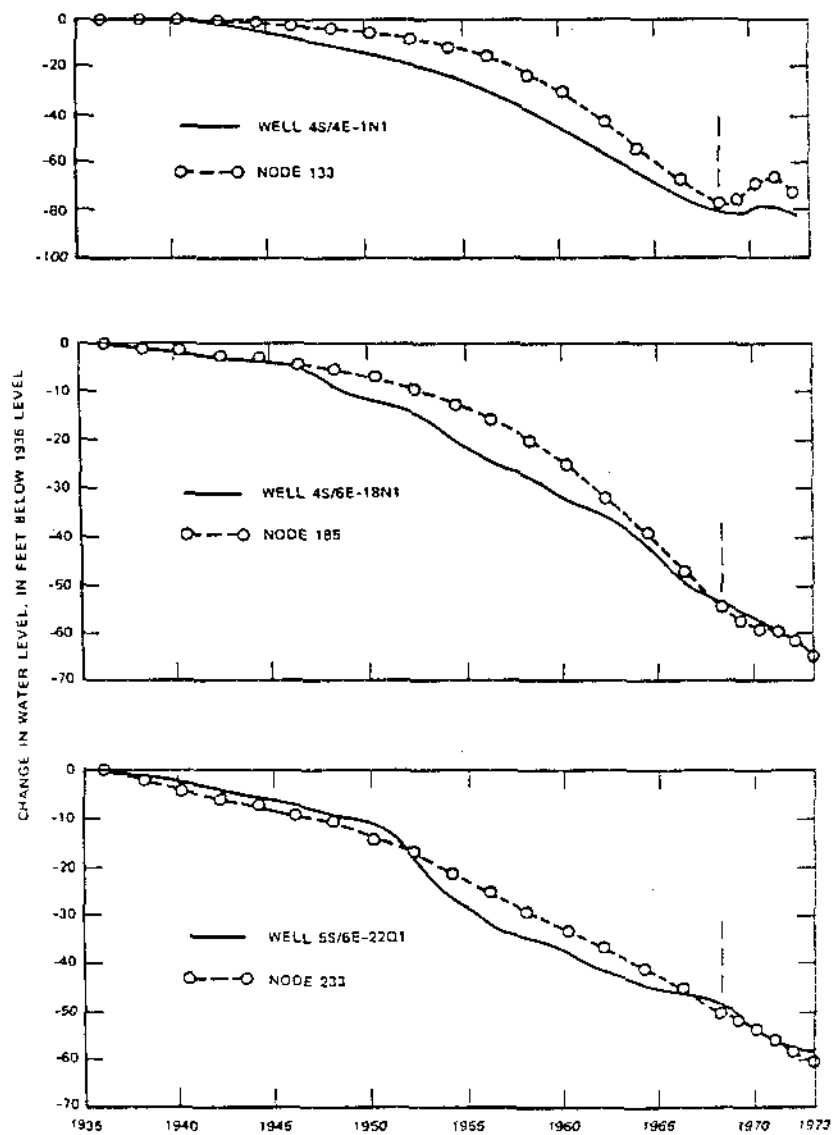
Figure 6. Comparison of measured and simulated water levels for Upper Coachella Valley groundwater basin model[14].
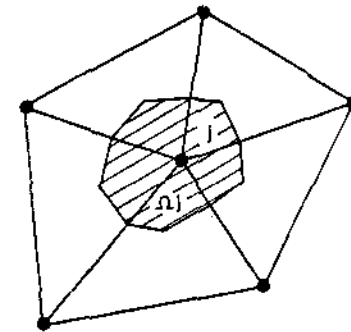

Figure 7. Subdomain Ω_j as the union of all nodal domains associated with node j.
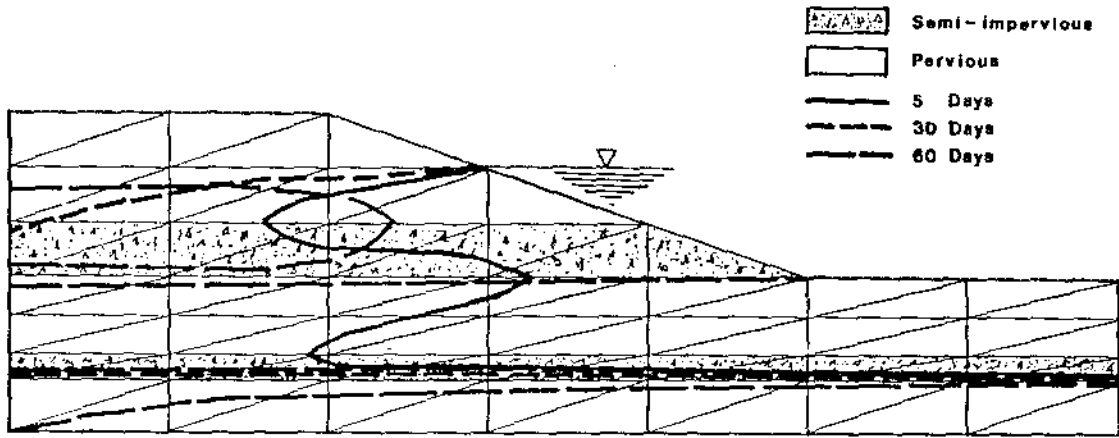
Figure 8. Nodal domain integration model of a floodwater detention basin showing water surfaces at various times after initial filling of basin.